CHAPTER 3

An Olefin Metathesis Route to the Preparation of Functionalized Hyperbranched Polymers

Portions of this chapter have previously appeared as: Gorodetskaya, I. A.; Gorodetsky, A. A.; Vinogradova, E. V.; Grubbs, R. H. *Macromolecules* **2009**, *42*, 2895-2898.

Abstract

A method for the post-synthetic functionalization of hyperbranched polymers prepared by olefin metathesis is reported. This modification is performed by a second metathesis step and can be used to introduce a variety of small molecules, including fluorophores, into the polymer's periphery. Hyperbranched macromolecules functionalized with pyrene demonstrate high local concentrations of the analyte relative to the unbound fluorophore. The comparison of the photophysical properties of the hyperbranched polymer decorated with pyrene to an analogous linear polymer suggests a different distribution of the analyte within the dendritic architecture.

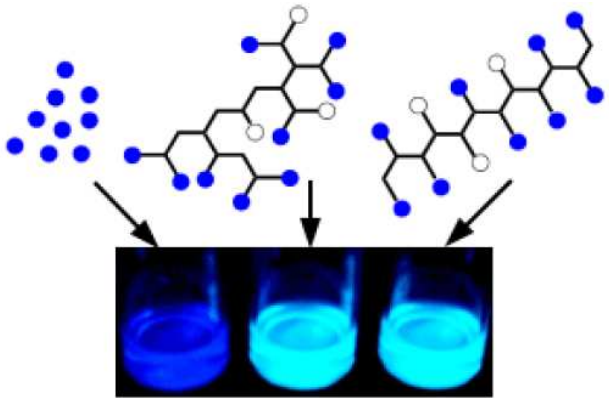

Introduction

Hyperbranched polymers are highly branched, three-dimensional macromolecules which are closely related to dendrimers and are typically prepared via a one-pot polycondensation of $AB_{n\geq 2}$ monomers.[1-6] Although hyperbranched macromolecules lack the uniformity of monodisperse dendrimers, they still possess many attractive dendritic features such as good solubility, low solution viscosity, globular structure, and multiple end-groups.[1-8] Furthermore, the usually inexpensive, one-pot synthesis of these polymers makes them particularly desirable candidates for both bulk-material and specialty applications. Toward this end, hyperbranched polymers have been investigated as both rheology-modifying additives to conventional polymers and as substrate-carrying supports or multifunctional macroinitiators, where a large number of functional sites within a compact space becomes beneficial.[1,2,7,9]

The properties of a polymeric material are considerably influenced by its end groups.[10] Compared to a linear polymer, this effect is more pronounced for a hyperbranched architecture simply because of a significantly larger number of end groups per single polymer chain (there is one end-group per every monomer) and their exposed placement (most of the ends are thought to be located on the periphery of the spherically-shaped units). In fact, it has been demonstrated that the chemical nature of the end-group functionalities of a hyperbranched polymer dominates not only the material's solubility in various solvents,[7,11-13] but also melt and thermal properties such as the glass transition temperature,[5,7,11-14] and crystallinity.[14] Consequently, it is desirable to have a simple, convenient, and modular method for post-synthetic functionalization of hyperbranched polymers.

Within the past 10 years, the development of new synthetic routes to hyperbranched polymers has surpassed the detailed investigation of these materials. As a result, a great variety of dendritic backbones is now available, while information on their physical properties, especially when compared to linear analogs, remains limited.[15] In particular, despite the importance of the end-groups for both property-tuning and substrate-carrying applications of hyperbranched polymers, little is known about the dendritic chain termini microenvironments and branch folding.[9,16]

Chapter 2 described a facile approach to the synthesis of hyperbranched polymers via acyclic diene metathesis polymerization (ADMET).[17] This method is based on the selectivity of N-heterocyclic carbene catalyst **1** (Figure 3.1) in the cross metathesis of different types of olefins. Since **1** promotes a selective reaction between an electron rich terminal aliphatic alkene and an electron poor acrylate, compounds such as AB_2 monomer **2** (Scheme 3.1) form highly branched structures such as **3** (Scheme 3.1) in its presence. Moreover, given that there are twice as many acrylates (B functionalities) as terminal alkenes (A functionalities) in the reaction mixture during the polymerization of **2**, half of the acrylates remain available for further manipulation.

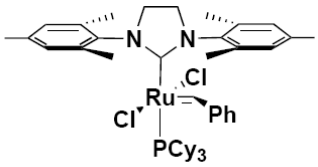

1

Figure 3.1. Imidazolinylidene-based ruthenium olefin metathesis catalyst **1**.

This chapter reports on the advances in the functionalization of **3** by a second cross metathesis reaction with a small fluorescent analyte—alkene modified pyrene. Although there have been numerous reports on the fluorescent properties of pyrene functionalized dendritic and linear macromolecules, these studies have typically focused on comparing polymers to small molecules.[18-27] Here, the information gathered from the comparison of the absorption and emission spectra of the decorated hyperbranched polymer with not only the spectra for a monomeric fluorophore but also the spectra of a similarly labeled linear polymeric analog can provide improved insight into the environment of the polymer's end-groups.

Results and Discussion

Functionalization of the Hyperbranched Polymer. Although a variety of chemical transformations can be employed in the functionalization of the terminal acrylates of **3**, olefin cross metathesis with **1** and an aliphatic alkene is the most advantageous route for several reasons. First, and most importantly, this selective reaction proceeds in

excellent yields and does not produce any non-volatile, stoichiometric by-products. Second, this method is inherently compatible with any functionality incorporated within the polymer backbone because it is the same reaction as the polymerization itself; notably, the synthesis and functionalization can be efficiently performed in tandem. Finally, substrates with functionalities not already present in the polymer can be introduced into the polymer because of the excellent functional group tolerance of **1**.

The cross metathesis functionalization of the end group acrylates was initially tested with a simple, commercially available aliphatic alkene—10-bromo-1-decene (Scheme 3.1). This molecule's molecular weight is very close to that of the monomer **2**, which aided the Size Exclusion Chromatography (SEC) analysis of the modified products. Since the hyperbranched polymer **3** has as many available end-groups as monomers in its backbone, complete functionalization with bromodecene should approximately double its molecular weight. However, only half of the necessary amount of the alkene was utilized to reduce the need for sample purification and further simplify the interpretation of SEC data. As can be seen from the SEC traces of the "before" and "after" samples in Figure 3.2, the modification of **3** with 0.5 equivalents of bromodecene proceeded to completion without any backbone degradation; the polymer's molecular weight increased from 4.73 kDa to 7.9 kDa. Importantly, thus functionalized **3** is susceptible to further manipulations by S_N2 chemistry of the peripheral bromine groups.

Scheme 3.1. Hyperbranched ADMET polymerization[17] and subsequent end group functionalization.

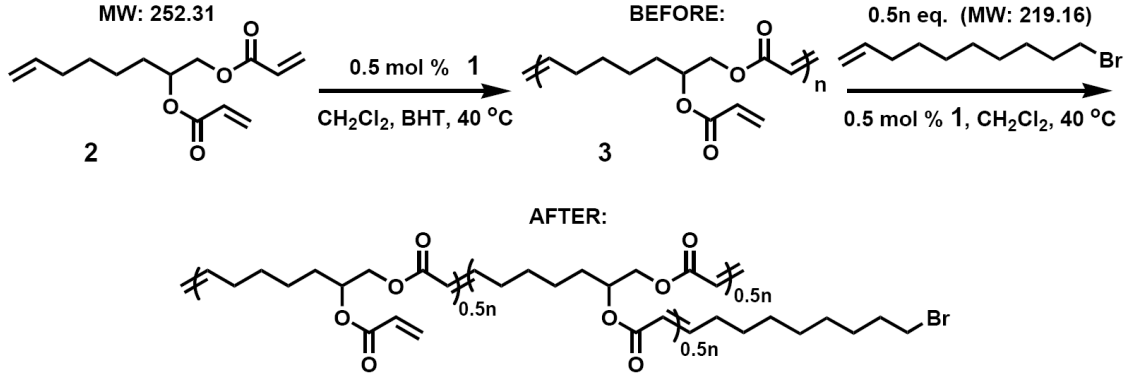

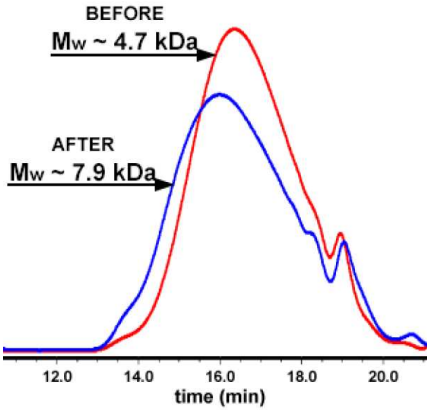

Figure 3.2. SEC (RI) traces for **3** before (red) and after (blue) functionalization with 0.5 equivalents of 10-bromo-1-decene.

Modified pyrene **4** (Scheme 3.2) was subsequently selected for functionalization of the hyperbranched polymer **3** due to its attractive fluorescent properties. Pyrene is recognized as a particularly useful handle for the study of polymer dynamics and structure in solution.[18-25] This well-studied fluorophore is characterized by long lifetimes and sensitive solvatochromic shifts.[26,27] Furthermore, pyrene is known to associate through π-stacking interactions at millimolar concentrations, leading to the formation of highly stable excimers with red shifted emission.[26,27] Consequently, this analyte allows for a ratiometric and quantitative measurement of pyrene-pyrene interactions, such as those resulting from a high local concentration of the substrate enforced by a covalent attachment to a polymeric backbone.[18-25] Therefore, the functionalization of dendritic end-groups with pyrene is instrumental for the study of their microenvironments.

Scheme 3.2. Hyperbranched polymer **3** functionalization with pyrene.

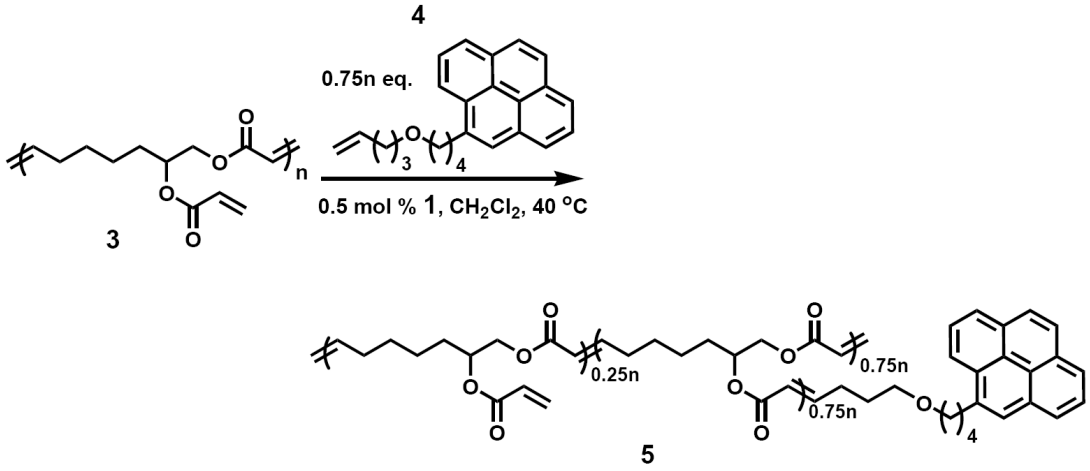

1-Pyrenebutanol was modified with an aliphatic alkene to produce **4**, which is suitable for selective cross metathesis with an acrylate and **1**. The functionalization method works according to the same principles as the polymerization itself: **1** selectively crosses the electron deficient acrylates with the electron rich alkene of **4**. Furthermore, this approach only affects the terminal acrylates, since the internal, di-substituted acrylates of the polymer backbone are too sterically hindered to participate in cross metathesis. In fact, if the internal acrylates could participate in the cross metathesis with **4**, degradation of the backbone would be unavoidable. However, the polymer modification proceeds to completion, and **5** is produced cleanly according to analysis by ^{1}H NMR and SEC (Figures 3.3 and 3.4).

The ^{1}H NMR spectra in Figure 3.3 show the polymerization progression of **2** to **3** and the subsequent modification of crude **3** with **4** (Scheme 3.2). In the spectrum of **2**, the peaks downfield of the solvent peak correspond to the six acrylate protons (**a**) and one terminal alkene proton (**d**). As polymer **3** is formed, all of the terminal alkenes of **2** are consumed (**d** disappears) and half of the free acrylates are internalized, thereby producing peaks **b** in the corresponding integration ratios.[17] Finally, when the remaining terminal acrylates of **3** are reacted with ~ 0.75 equivalents (per end group) of **4**, the amount of free acrylates is reduced to ~ 0.25 equivalents (for each peak **a**). Consequently, ~ 0.75 equivalents of internal, pyrene-functionalized acrylates (for each peak **c**) are added to the existing internal acrylates within the polymer backbone (1 equivalent for each peak **b**). As

expected, the integration values for the backbone protons **e** of **2** remain constant throughout all of these transformations (Figure 3.3). However, although the presented ^{1}H NMR analysis strongly supports successful functionalization of **3**, it provides little definitive information on the integrity of the polymer's backbone.

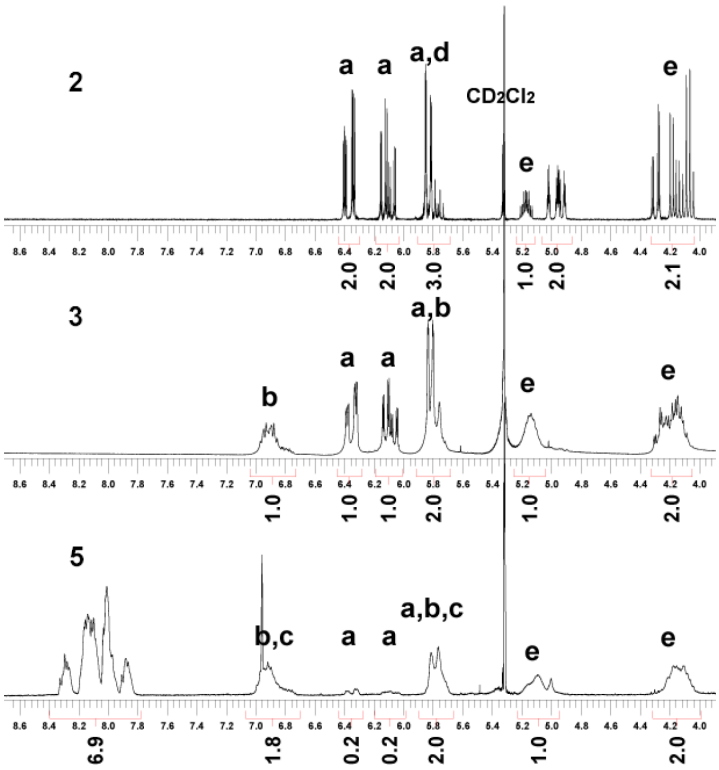

Figure 3.3. ^{1}H NMR spectra with integration values for **2**, **3**, and **5**. Peaks **a** correspond to the protons of the free terminal acrylate groups. Peaks **b** correspond to the protons of the internal acrylates within the polymer backbone. Peaks **c** correspond to the protons of the internal acrylates resulting from functionalization with **4**. Peak **d** is due to the proton of the terminal alkene of **2** (which is consumed during the polymerization), and peaks **e** correspond to the backbone protons of **2**.

Figure 3.4 compares the SEC traces of the polymer before (**3**) and after functionalization with **4** (**5**). Although crude **3** (purple trace) was used in the functionalization studies, the resulting **5** (pink trace) was later purified (red trace) for further fluorescence investigations. In spite of the broad polydispersity typical of hyperbranched polymers, the evaluation of the SEC traces obtained for crude **3** and **5** clearly demonstrates that no observable backbone degradation occurs as a result of functionalization. Moreover, the absolute molecular weight corresponding to the major

peak of **5** (M_w ~ 7.87 kDa, measured by a triple angle light scattering technique) is approximately double that of the major peak of **3** (M_w ~ 3.33 kDa), which is in agreement with the postulate that ~ 75% of the end groups of **3** have reacted with **4** (Figure 3.4). In addition, as expected for a compact dendritic architecture, only a very slight elution time shift is observed for **5** relative to **3** despite the significant molecular weight difference between the two. Overall, both ^{1}H NMR and SEC analysis indicate that only free, terminal acrylates participate in the post-synthetic functionalization of hyperbranched polymer **3**.

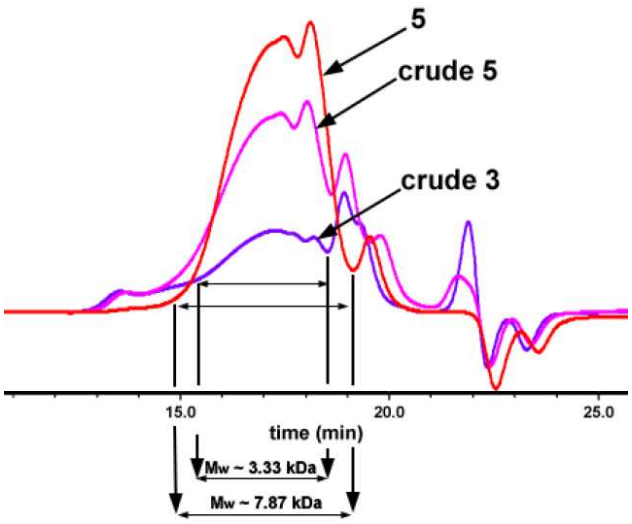

Figure 3.4. SEC (RI) traces for crude **3** (purple), crude (pink) and purified (red) **5**. The molecular weight of the major peak is approximately doubled after functionalization.

Preparation of the Pyrene Modified Linear Analog. Another significant advantage of the olefin metathesis route to the synthesis and functionalization of hyperbranched polymers is that very similar linear polymers can be prepared via the same methodology. This aspect of the synthetic strategy outlined here is crucial for the direct comparison of hyperbranched polymers to suitable linear analogs. Moreover, there is more than one way to approach this task, as either ADMET of AB monomers[17] or ring opening metathesis polymerization (ROMP) of appropriately functionalized cyclic monomers can be utilized.

We chose to prepare our linear analog by ROMP of pyrene-functionalized cyclooctene (**6**), in order to simplify the molecular weight control over the polymerization reaction (Scheme 3.3). Since ROMP is a chain-growth type polymerization which relies on

monomer ring strain, it can be simply and efficiently controlled by the catalyst loading. In addition, to ensure that the linear polymer had a similar pyrene-per-chain content as the hyperbranched version, **6** was co-polymerized with a corresponding amount of "blank" methoxy-functionalized monomer **7**. The resulting random co-polymer **8** had approximately 75 pyrenes per 100 monomers, as did the hyperbranched polymer **5** (Figure 3.5).

Scheme 3.3. Synthesis of the pyrene-functionalized linear polymeric analog.

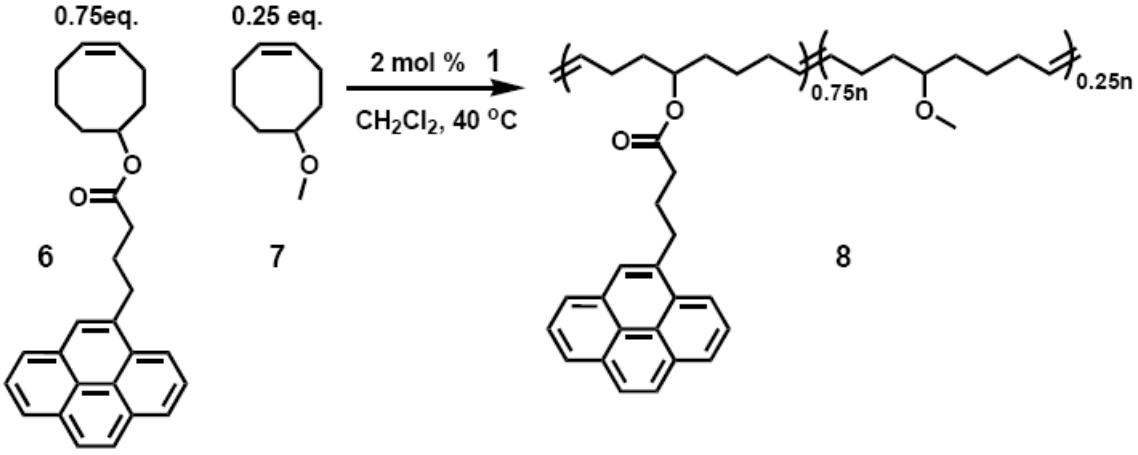

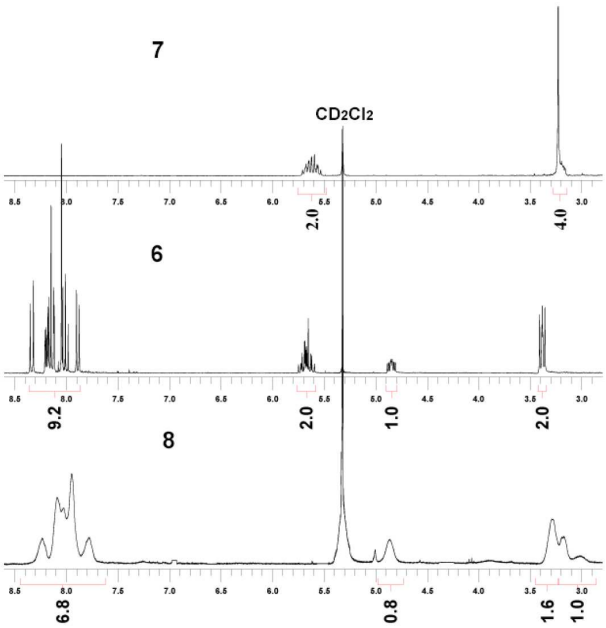

Figure 3.5. ^{1}H NMR spectra with integration values for **6**, **7**, and **8**.

Fluorescence Properties of Pyrene-Functionalized Hyperbranched and Linear Polymers. Figure 3.6A compares the UV-visible absorbance and steady-state fluorescence emission spectra for solutions of monomeric pyrene **4**, pyrene-functionalized hyperbranched polymer **5**, and similarly functionalized linear analog **8**. The normalized UV-Vis spectra of all three compounds overlap almost perfectly with no observed spectral broadening or red shift of the linear and hyperbranched polymer (relative to the pyrene monomer). This indicates that the polymeric scaffold does not dramatically influence the interaction of the pyrene moieties in the ground state. On the other hand, the fluorescence emission spectra of the three compounds at the identical concentrations are quite distinct. For all three samples, peaks which correspond to emission from the monomeric pyrene are evident at 380 nm and 400 nm. In addition, for the hyperbranched polymer **5** and linear analog **8**, a broad and featureless excimer emission centered at 480–500 nm is also evident. Therefore, the pyrene moieties must interact strongly in the excited state due to constraints imposed by the backbones of **5** and **8**.

As can be seen in Figure 3.6B, the ratios of the monomer to excimer emission intensity indicate that the degree of pyrene association is different for **5** and **8**. At a low pyrene concentration of ~ 80 μM, the ratio of the excimer to monomer emission intensity (I_E/I_M) is 1.5 for the hyperbranched polymer and 7.9 for the linear analog. As expected, no stacking is observed for free pyrene **4** at micromolar concentrations. For both **5** and **8**, over the concentration range tested, there is only a slight change in the excimer to monomer ratio, indicating that the pyrene interactions are intramolecular rather than intermolecular. Therefore, although both polymers do serve to effectively increase the local pyrene concentration, the hyperbranched architecture promotes stacking less effectively than the linear scaffold. Given the nearly identical backbone chemical compositions, concentrations, and degrees of functionalization for samples **5** and **8**, these observations suggest that some of the pyrene moieties are confined to the interior of the hyperbranched polymer and are, thus, shielded from adjacent pyrenes.

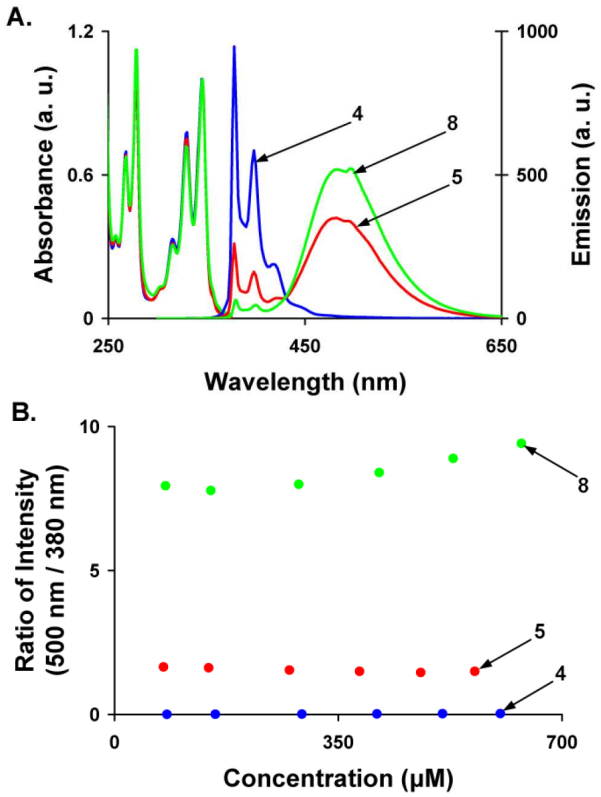

Figure 3.6. **(A)** UV-visible absorbance and fluorescence emission spectra for **4** (blue), **5** (red), and **8** (green) in dichloromethane. The absorbance spectra have been normalized for clarity, and the fluorescence spectra were obtained at an 80 μM concentration. **(B)** A plot of the monomer (380 nm) to excimer (500 nm) intensity emission ratio at various concentrations.

Conclusion

In conclusion, hyperbranched polymers were prepared via ADMET with catalyst **1** and efficiently functionalized at their periphery by further cross metathesis. This strategy should prove general for the post-polymerization modification of ADMET hyperbranched polymers with a variety of terminal alkene modified substrates. Moreover, this simple olefin metathesis approach to the synthesis of functionalized hyperbranched polymers can be easily extended to the preparation of linear analogs, which are useful for the investigations of the influence of different polymeric architectures on material properties. In particular, our studies of pyrene-functionalized hyperbranched and linear polymers showed that while both polymeric backbones enforce higher local concentrations of a bound fluorophore relative to its free form, only the hyperbranched scaffold appears to partially shield the analytes from each other, possibly through absorption into the dendritic

interior. These observations may hold implications for the use of hyperbranched polymers as drug-delivery systems.[28]

Experimental Procedures

Materials. All reagents, except for catalyst **1** and 1-pyrenebutyric acid were purchased from Aldrich at the highest available purity and used without further purification. Catalyst **1** was obtained from Materia, Inc., and 1-pyrenebutyric acid (≥97%) was purchased from Fluka. The synthesis of **2** and its polymerization to **3** with **1** have been reported previously.[17]

Instrumentation. NMR spectra were obtained using a Varian Mercury-300 spectrometer; samples were dissolved in CD_2Cl_2.

Size exclusion chromatography (SEC) analysis was performed using a Wyatt triple detector system equipped with a triple angle light scattering (miniDAWN TREOS, with laser wavelength of 658 nm) detector, a viscometer (ViscoStar) detector, and a refractive index (Optilab rEX) detector—all operating at 25°C. Viscotek ViscoGEL I-Series (one mixed bed medium MW and one mixed bed high MW) columns were used for SEC with THF as the eluent and a Shimadzu LC-10AD pump operating at 1 mL/minute.

Fluorescence measurements were conducted using an ISS K2 fluorimeter (5 mm path length), equipped with a 250 W xenon lamp as excitation source. Emission spectra were obtained by exciting at 346 nm and monitoring the emission between 300 and 700 nm. UV-Vis spectra were recorded on a Beckman DU 7400 spectrophotometer.

Synthesis of 4-(4-pent-4-enyloxy-butyl)-pyrene (4). 1-Pyrenebutanol (1.0 g, 3.6 mmol) was combined with potassium hydride (35% suspension in oil, 1 g, 8.7 mmol) in 10 mL of toluene in a 50 mL round bottom flask equipped with a stir bar. The solution was stirred at room temperature until it had stopped evolving gas, at which point 5-bromo-pentene (0.6 mL, 5 mmol) was slowly added to the reaction flask. The reaction was subsequently heated to reflux for 10 h. The reaction mixture was then cooled to room temperature, and the unreacted potassium hydride was neutralized with a small amount of iPrOH before the solution was filtered and concentrated. The product was purified by silica gel chromatography, eluting with 5% EtOAc in hexane, and recrystallized from cold (0°C) hexane to give a quantitative yield of pure **4** as a yellowish crystalline solid. ^{1}H NMR (300 MHz, CD_2Cl_2, ppm): 8.32 (d, J = 9 Hz, 1H), 8.19–7.97 (m, 7H), 7.90 (d, J = 7.8 Hz, 1H), 5.83 (m, 1H), 5.04–4.91 (m, 2H), 3.49–3.35 (m, 6H), 2.09 (m, 2H), 1.93 (m, 2H),

1.79–1.59 (m, 4H). ^{13}C NMR (300 MHz, CD_2Cl_2, ppm): δ 139.17, 137.80, 131.99, 131.50, 129.33, 128.04, 127.89, 127.58, 126.99, 126.37, 125.49, 125.33, 125.18, 125.04, 124.11, 114.82, 71.08, 70.66, 33.81, 30.95, 30.40, 29.62, 29.11.

Synthesis of pyrene functionalized hyperbranched polymer (5). **3** (163 mg, 0.646 mmol in monomer), **4** (167 mg, 0.485 mmol, 0.75 equivalents), and **1** (3 mg, 3.53 μmol) were combined in 2 mL of dry CH_2Cl_2 under an inert atmosphere. The reaction mixture was stirred at 40ºC for 10 h with venting through a bubbler. Subsequently, the reaction was concentrated and the product was characterized by ^{1}H NMR spectroscopy with no further purification. NMR analysis indicated clean and complete addition of all of the added **4** (0.75 equivalents per repeat unit in **3**).

Scheme 3.4. Synthesis of the monomers for linear ROMP.

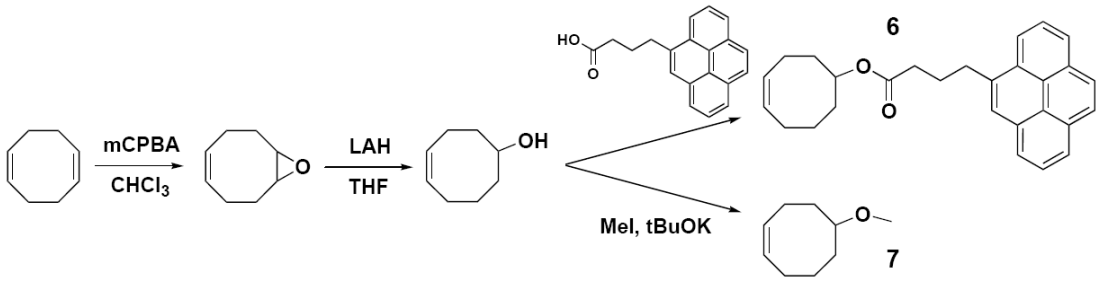

Synthesis of linear pre-monomer, cyclooct-4-enol. A 250 mL round bottom flask equipped with a stir bar and an addition funnel was charged with 1,5-cyclooctadiene (8.6 g, 79.1 mmol). The solution of mCPBA (11.1 g, 64.1 mmol) in chloroform (180 mL) was added to the reaction flask drop-wise via the addition funnel (Scheme 3.4). The reaction mixture was stirred for 10 h and then filtered; it was then washed with aqueous solutions of $NaHSO_3$ (3 times), $NaHCO_3$ (once), and brine (once) consequently. The purification by silica gel chromatography, eluting with 10% EtOAc in hexane, gave 4.2 g (43% yield) of the epoxide product. ^{1}H NMR (300 MHz, CD_2Cl_2, ppm): δ 5.57 (m, 2H), 3.00–2.95 (m, 2H), 2.46–2.36 (m, 2H), 2.18–1.93 (m, 6H). ^{13}C NMR (300 MHz, CD_2Cl_2, ppm): δ 129.35, 56.95, 28.68, 24.20.

A 1M THF solution of LAH (17.0 mL, 17.0 mmol) was slowly added to the solution of the epoxide (4.21 g, 33.9 mmol) in THF (23 mL) at room temperature and the mixture was stirred for 10 h (Scheme 3.4). The reaction was then quenched with sodium

sulfate decahydrate, stirred very well for 20 minutes, filtered through Celite, and concentrated. The purification by silica gel chromatography with a 30% EtOAc in hexane eluent afforded 4.0 g (95% yield) of a clear colorless oil. ^{1}H NMR (300 MHz, CD_2Cl_2, ppm): δ 5.73–5.53 (m, 2H), 3.75 (m, 1H), 2.33–2.23 (m, 2H), 2.17–2.03 (m, 2H), 1.94–1.75 (m, 2H), 1.71–1.44 (m, 4H). ^{13}C NMR (300 MHz, CD_2Cl_2, ppm): δ 130.67, 129.95, 73.09, 38.29, 36.92, 26.13, 25.47, 23.30.

(**6**). Cyclooct-4-enol (0.3 g, 2.4 mmol), 1-pyrenebutyric acid (1.0 g, 3.5 mmol), DMAP (0.6 g, 4.8 mmol), and Et_3N (1.3 mL, 9.5 mmol) were dissolved in 10 mL of dry methylene chloride (Scheme 3.4). 2,4,6-Trichlorobenzoyl chloride (1.16 g, 4.8 mmol) was then slowly added to the reaction mixture, and the reaction was stirred for 10 h. The unreacted benzoyl chloride was neutralized with a small amount of iPrOH before the solution was filtered and concentrated. The product was then purified by silica gel chromatography, eluting with 5% EtOAc in hexane, to give 0.9 g (95% yield) of a semi-crystalline, bright yellow material. ^{1}H NMR (300 MHz, CD_2Cl_2, ppm): δ 8.33 (d, J = 9.6, 1H), 8.21–7.98 (m, 7H), 7.89 (d, J = 8.1, 1H), 5.76–5.60 (m, 2H), 4.86 (m, 1H), 3.38 (t, J = 7.6, 2H), 2.44–2.29 (m, 4H), 2.22–2.08 (m, 4H), 1.98–1.56 (m, 6H). ^{13}C NMR (300 MHz, CD_2Cl_2, ppm): δ 173.04, 136.77, 131.98, 131.49, 130.47, 130.34, 130.20, 129.28, 128.02, 128.00, 127.77, 127.15, 126.43, 125.54, 125.45, 125.42, 125.37, 125.28, 124.01, 76.01, 34.83, 34.33, 33.30, 28.45, 27.54, 26.14, 25.49, 22.88.

(**7**). Cyclooct-4-enol (0.5 g, 4.0 mmol) was combined with tBuOK (0.7 g, 6.0 mmol) in dry THF (8 mL) (Scheme 3.4). Upon addition of MeI (0.4 mL, 6 mmol) the reaction mixture was stirred at 35 ^{o}C for 10 h. The remaining unreacted tBuOK was neutralized with a small amount of iPrOH before the solution was filtered and concentrated. Purification by silica gel chromatography, eluting with 5% EtOAc in hexane, afforded 0.15 g (27% yield) of clear colorless oil **7**. ^{1}H NMR (300 MHz, CD_2Cl_2, ppm): δ 5.71 (m, 2H), 3.23 (s, 3H), 3.20 (m, 1H), 2.39–2.27 (m, 2H), 2.17–1.36 (m, 8H)
^{13}C NMR (300 MHz, CD_2Cl_2, ppm): δ 130.67, 129.90, 82.52, 56.15, 34.48, 33.33, 26.31, 26.20, 23.17.

Synthesis of pyrene functionalized linear polymer (8). Monomers **6** (100 mg, 0.25 mmol) and **7** (12.0 mg, 0.08 mmol) were dissolved in dry CH_2Cl_2 (1 ml) under an argon atmosphere. Catalyst **1** (5 mg, 6 μmol) was added to the reaction flask, and the solution was stirred at 45ºC for 24 hours. Upon consumption of the monomers, the volatiles were removed under reduced pressure. The product was then redissolved in a small amount of CH_2Cl_2, loaded on a short silica plug, rinsed with CH_2Cl_2, and eluted with THF. The purified product was characterized by ^1H NMR spectroscopy and triple detector–SEC (M_w ~ 38K, M_w/M_n ~ 1.45).

References

(1) Voit, B. *J. Polym. Sci., Part A: Polym. Chem.* **2005**, *43*, 2679-2699.

(2) Yates, C. R.; Hayes, W. *Eur. Polym. J.* **2004**, 1257-1281.

(3) Voit, B. I. *C. R. Chimie* **2003**, *6*, 821-832.

(4) Voit, B. *J. Polym. Sci., Part A: Polym. Chem.* **2000**, *38*, 2505-2525.

(5) Hult, A.; Johansson, M.; Malmström, E. *Adv. Polym. Sci.* **1999**, *143*, 1-34.

(6) Kim, Y. H. *J. Polym. Sci., Part A: Polym. Chem.* **1998**, *36*, 1685-1698.

(7) Wooley, K. L.; Hawker, C. J.; Lee, R.; Fréchet, J. M. J. *Polymer J.* **1994**, *26*, 187-197.

(8) Wooley, K. L.; Fréchet, J. M. J.; Hawker, C. J. *Polymer* **1994**, *35*, 4489-4495.

(9) Johansson, M.; Malmström, E.; Hult, A. *Trends in polymer science* **1996**, *4*, 398-403.

(10) *Cyclic Polymers*; 2nd ed.; Semlyen, J. A., Ed.; Kluwer Academic Publishers: Dordrecht, The Netherlands, 2000.

(11) Kim, Y. H.; Webster, O. W. *Macromolecules* **1992**, *25*, 5561-5572.

(12) Uhrich, K. E.; Hawker, C. J.; Frechet, J. M. J.; Turner, S. R. *Macromolecules* **1992**, *25*, 4583-4587.

(13) Hawker, C. J.; Chu, F. *Macromolecules* **1996**, *29*, 4370-4380.

(14) Malmström, E.; Johansson, M.; Hult, A. *Macromol. Chem. Phys.* **1996**, *197*, 3199-3207.

(15) Stiriba, S. E.; Kautz, H.; Frey, H. *J. Am. Chem. Soc.* **2002**, *124*, 9698-9699.

(16) Lescanec, R. L.; Muthukumar, M. *Macromolecules* **1990**, *23*, 2280-2288.

(17) Gorodetskaya, I. A.; Choi, T. L.; Grubbs, R. H. *J. Am. Chem. Soc.* **2007**, *129*, 12672-12673.

(18) Winnik, M. A.; Bystryak, S. M.; Liu, Z.; Siddiqui, J. *Macromolecules* **1998**, *31*, 6855-6864.

(19) Baker, L. A.; Crooks, R. M. *Macromolecules* **2000**, *33*, 9034-9039.

(20) Brauge, L.; Caminade, A. M.; Majoral, J. P.; Slomkowski, S.; Wolszczak, M. *Macromolecules* **2001**, *34*, 5599-5606.

(21) Gao, C.; Yan, D.; Zhang, B.; Chen, W. *Langmuir* **2002**, *18*, 3708-3713.

(22) Chen, J.; Jiang, M.; Zhang, Y.; Zhou, H. *Macromolecules* **1999**, *32*, 4861-4866.

(23) Wilson, J. N.; Teo, Y. N.; Kool, E. T. *J. Am. Chem. Soc.* **2007**, *129*, 15426-15427.

(24) Ingratta, M.; Duhamel, J. *Macromolecules* **2007**, *40*, 6647-6657.

(25) Ingratta, M.; Hollinger, J.; Duhamel, J. *J. Am. Chem. Soc.* **2008**, *130*, 9420-9428.

(26) Winnik, F. M. *Chem. Rev.* **1993**, *93*, 587-614.

(27) Klessinger, M.; Michl, J. *Excited States and Photochemistry of Organic Molecules*; VCH: New York, N. Y., 1995.

(28) Paleos, C. M.; Tsiourvas, D.; Sideratou, Z. *Mol. Pharmaceutics* **2007**, *4*, 169-188.